INFLUENCE OF QUALITY OF MECHANICAL SPLICES ON BEHAVIOR OF REINFORCED CONCRETE MEMBERS

Dac Phuong NGUYEN [1)] and Hiroshi Mutsuyoshi [1)]
[1)] Structural Material Lab., Department of Civil and Environmental Engineering, Saitama University

ABSTRACT

Mechanical splices are commonly used on site to join two steel reinforcing bars. Although quality of mechanical splices is ensured by manufacturers but the low quality splices still appear in construction sites due to the improper installation of the splices. This study investigates properties of improperly installed mechanical splices and their influence on the behavior of RC beams. The test results show that the improperly installed mechanical splices have lower performance in stiffness, tensile strength and elongation than those of the plain steel bar. RC beams using improperly installed mechanical splices have lower behavior in load carrying capacity, ductility and cracking compared to the beam using perfect mechanical splices or the control beam without mechanical splices. A corrective splice for improving improperly installed mechanical splices is newly developed. Mechanical properties as well as their influences on the behavior of RC beams of the improperly installed mechanical splices are confirmed to be improved through tensile tests and beam tests of specimens using corrective splices fitting over the improperly installed mechanical splices.

KEYWORDS: reinforced concrete, mechanical splice, corrective splice

1. INTRODUCTION

Length of the reinforcing bar is limited by fabricating, transporting or storage capacity and normally supplied in standard stock length (commonly known as mill length). As a result, the mill length of steel bars could not ensure the integrity of throughout any sizeable structures. Therefore, splicing reinforcing bars is unavoidable.

Basically, there are four kinds of splice included lap splice, mechanical splice, welded splice and gas pressure welding splice (Figure 1).

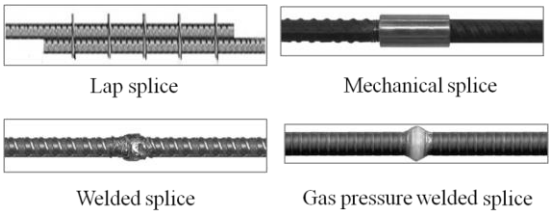

Figure 1. Splice of reinforcing bars

Among these four kinds of splice, mechanical splice is used popularly in construction of RC structures. For using mechanical splices, the principal is that mechanical splices should not decrease the load bearing capacity, ductility and stiffness of the structures compared to the structures without splices. It means that using mechanical splices does not create weak points affecting the performance of the structures. Mechanical splices are now produced satisfying the requirements on load carrying capacity, ductility and stiffness of the reinforced concrete members. However, during the installation process, mechanical splices may not achieve the quality as expected. The properties of such mechanical splices and their effect on behavior of reinforced concrete members have been hardly clarified. There are numerous studies about mechanical splices focusing on mechanical properties of mechanical splices, developing new mechanical splices or effect of mechanical splices on the behavior of the structures. However, there is no research on improperly installed mechanical splices. The objective of this study is to investigate the performance of improperly installed mechanical splices and develop a corrective splice for improving such mechanical splices.

2. PROPERTIES OF IMPROPERLY INSTALLED MECHANICAL SPLICES

2.1. Specimens and test set up

Six different mechanical splices were subjected to tensile tests; the variations consisted of different bar embedment lengths in the coupler and the use or not of injected epoxy in the coupler. Specimen MS-6me is a correctly installed splice with the correct embedment (6 threads) and injected epoxy. Specimen MS-6m has the same

embedment length as specimen MS-6me but lacks the epoxy resin. Specimens MS-2me and MS-3me have embedment lengths of 2 threads and 3 threads, respectively, and are injected with epoxy resin. Specimens MS-2m and MS-3m have the same embedment lengths as specimen MS-2me and MS-3me, respectively, but lack the epoxy resin. Details of the specimens are given in Figure 2.

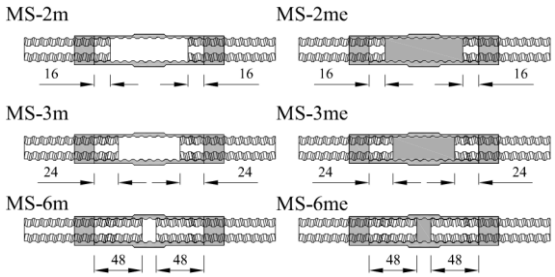

Figure 2. Tensile test specimens

The test setup is shown in Figure 3. Steel bar and coupler strains were measured using strain gauges attached along the specimen. Elongation of 180 mm length between two points outside the two nuts of the mechanical splices was measured with a pair of linear variable differential transformer (LVDT) accompany with a measuring frame. Tensile load is applied monotonically until the steel bar ruptured or slipped out of the coupler.

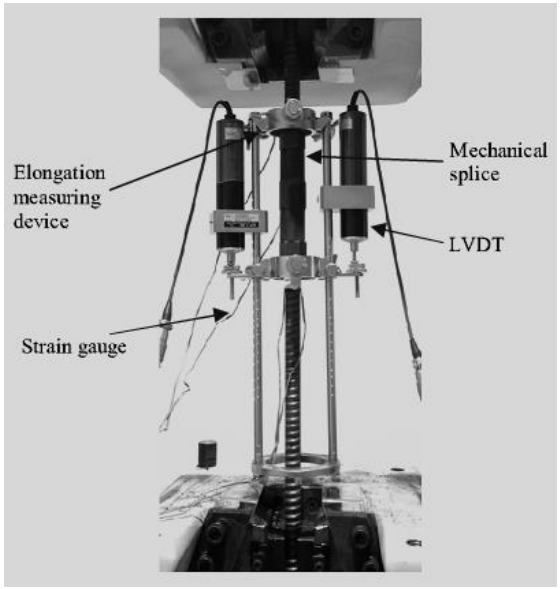

Figure 3. Tensile test set-up

2.2. Test results

The test results including stress-strain curves, tensile strength and failure modes are taken into account. Table 1 describes the tensile strength and failure mode of each specimen. All specimens with insufficient embedment in the coupler (MS-3me, MS-3m, MS-2me, and MS-2m) had lower performance compared to the D19 bar.

Table 1. Tensile test results

	f_y N/mm^2	f_u N/mm^2	f_u/ $f_{y(D19)}$	Failure mode
D19 bar	380	546	144%	Bar rupture
MS-2m	-	240	63%	Slippage
MS-2me	-	357	94%	Slippage
MS-3m	380	451	119%	Slippage
MS-3me	380	444	117%	Slippage
MS-6m	380	558	147%	Bar rupture
MS-6me	380	556	146%	Bar rupture

Figure 4 shows the stress-strain curves of the specimens. Strains are values obtained by dividing the measured elongation by the original length (180 mm) before the test. The stress was calculated by dividing the load by the nominal area of the D19 bar (286.2 mm^2). Slippage of the bar from the mechanical splice is indicated by a difference in the stress versus apparent strain curves between the mechanical splice and the D19 steel bar. Specimen MS-6me (with 6 threads and epoxy injection) exhibited almost the same values of initial stiffness and strength as the plain D19 bar. Specimen MS-6m (6 threads and no epoxy resin) has lower initial stiffness than the D19 bar but with the same strength. All specimens with insufficient embedment in the coupler (MS-3me, MS-3m, MS-2me, and MS-2m) had lower performance compared to the D19 bar. Specimens MS-3m and MS-3me with 3 threads of embedment achieved the yield strength of the D19 bar but with lower stiffness, ultimate load, and elongation. The stiffness and elongation of specimen MS-3me are improved compared to specimen MS-3m due to the effect of the epoxy injection in the coupler. Ultimate loads of specimens MS-3m and MS-3me are approximately 119% of the yield strength of the D19 bar, which are smaller than the ultimate strength of the D19 bar (equal to 143%). Therefore, these two specimens failed due to slippage of the steel bars from the couplers, not rupture of the steel bars. Specimen MS-2m could develop only 64% of the yield strength of the D19 bar and its stiffness was very low. On the other hand, specimen MS-2me had 95% of the yield strength of the D19 bar, exceeding that of specimen MS-2m by 31%. Its stiffness is also higher than that of specimen MS-2m. In spite of these strength results, however, all mechanical splices exhibited smaller elongation compared to the D19 bar.

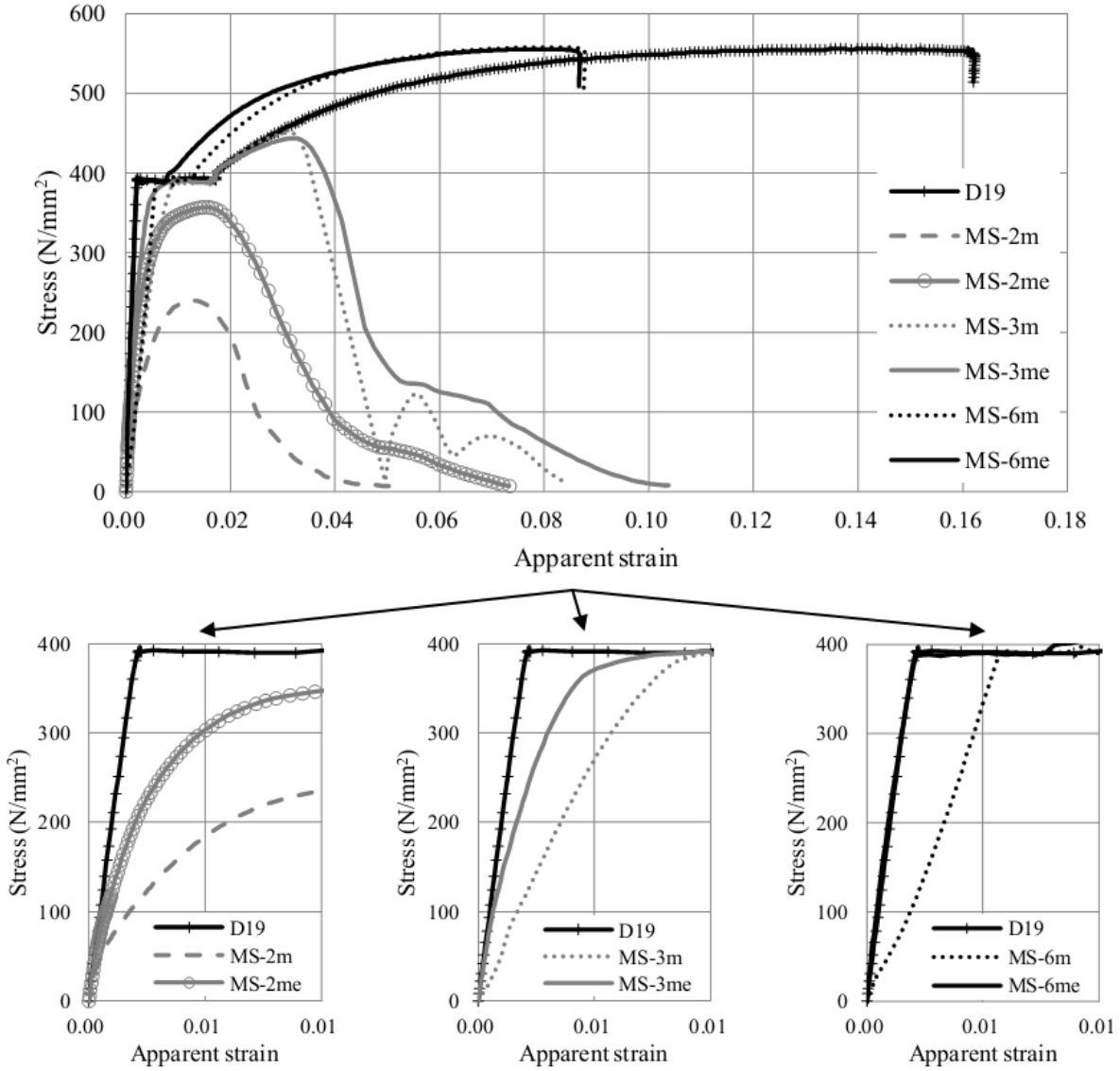

Figure 4. Stress-strain curves of mechanical splices

3. RC BEAMS USING IMPROPERLY INSTALLED MECHANICAL SPLICES

3.1 Specimens and test set up

Ten RC beams were prepared using mechanical splices with various embedment lengths and staggered by various distances. All beams were 3.0 m in length with a span of 2.5 m and a square cross section of 0.30 m. Figure 4 gives details of the test beam dimensions and the test set-up. Four longitudinal D19 steel bars were used and D10 bars were used as the stirrups at 100 mm spacing. Mechanical splices were located in the 800 mm uniform bending moment region. No stirrups were used in this region so as not to disturb the crack patterns.

According to the ACI 318-05 code, mechanical splices do not need to be staggered if they develop at least 125 percent of the yield strength of the bar. This requirement is normally satisfied by the manufacturer of a mechanical splice. Meanwhile, JSCE's Standard is stricter in stipulating that mechanical splices must be staggered in the longitudinal direction by at least the sum of the splice length (l) and 25 times the bar diameter (d). In this experiment, mechanical splices were staggered by three different amounts: 585 mm equals (25d+l), 348 mm equals (12.5d+l), and at the center of the span (no staggering). Table 2 provides a summary of the test beams.

The strains of the steel bars and concrete at the extreme compression surface were measured using strain gauges. Displacements were measured with LVDTs. Crack patterns were observed and crack widths were measured within the constant moment region using PI-shaped displacement transducers.

All beams were subjected to 30 cycles of loading at each load amplitude of 0.5Psy, 0.7Psy, and 0.95Psy (Psy: calculated yield load), and then until failure.

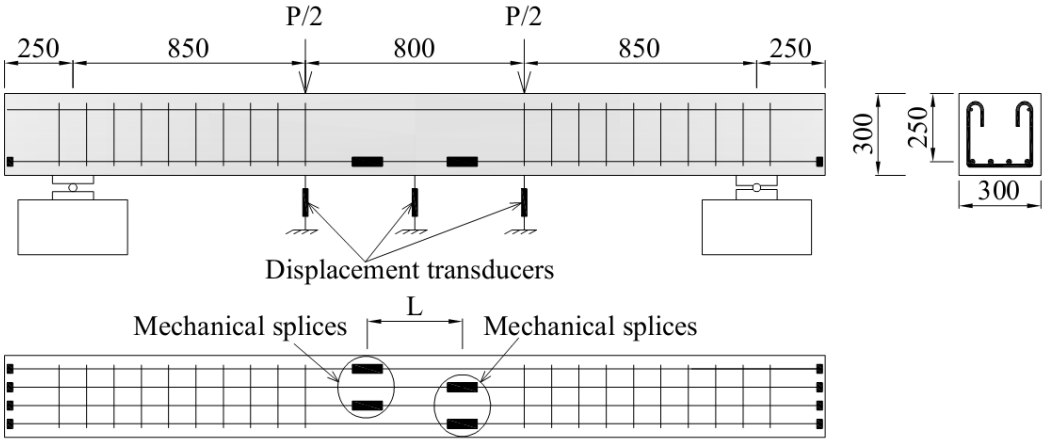

Figure 4. Beam configurations and test set up

Table 2 - Beam specimens

Beam	Concrete strength f'c, MPa	Mechanical splice type	Stagger distance L, mm
B1	36.2	-	-
B2-2m-0d	38.3	MS-2m	0
B3-2m-12.5d	37.9	MS-2m	348 (12.5d+l)
B4-2m-25d	37.0	MS-2m	585 (25d+l)
B5-3m-0d	36.8	MS-3m	0
B6-3me-0d	33.8	MS-3me	0
B7-3m-12.5d	34.3	MS-3m	348 (12.5d+l)
B8-3m-25d	34.6	MS-3m	585 (25d+l)
B9-6m-0d	33.8	MS-6m	0
B10-6me-0d	31.5	MS-6me	0

3.2 Test results

3.2.1. Load-displacement curves

Figure 5 shows the load–displacement curves of the test beams. Control beam B1 exhibits a typical flexural load-displacement relationship, including four different segments separated by four significant events: 1) flexural cracking (A); 2) yielding of tensile reinforcement (B); 3) crushing with associated spalling of concrete cover in the compression zone (C); and 4) disintegration of compressed concrete (D).

The behavior of the beams fabricated with sufficiently embedded splices (beams B9-6m-0d, B10-6me-0d) was almost the same as that of the control beam. They attained the same load carrying capacity as the control beam and failed by crushing of the concrete in compression after reaching almost the same displacement.

Beams B5-3m-0d, B6-3me-0d, B7-3m-12.5d, B8-3m-25d, in which the embedded length of bars was 3 threads, exhibited the same load carrying capacity as the control beam, while ultimate displacements were smaller than that of the control beam. In these beams, the bars slipped out from the coupler one thread at a time. The steel bars first slipped out of the coupler by one thread; a sudden fall in the load then followed. As loading continued, the beams were then able to sustain load before failure.

With beams B2-2m-0d, B3-2m-12.5d, B4-2m-25d, in which the embedded length of the bars was 2 threads, the yield strength of the steel bars could not be reached because failure of the mechanical splices occurred first. The load carrying capacities of these beams were much lower than that of the control beam. After the steel bars slipped from the couplers, beam B2-2m-0d with MS-2m splices all located in the same cross section was unable to bear any load. Meanwhile, beams B3-2m-12.5d, B4-2m-25d with staggered MS-2m splices still had some load carrying capacity before complete failure. The failure modes of these beams were sudden and brittle.

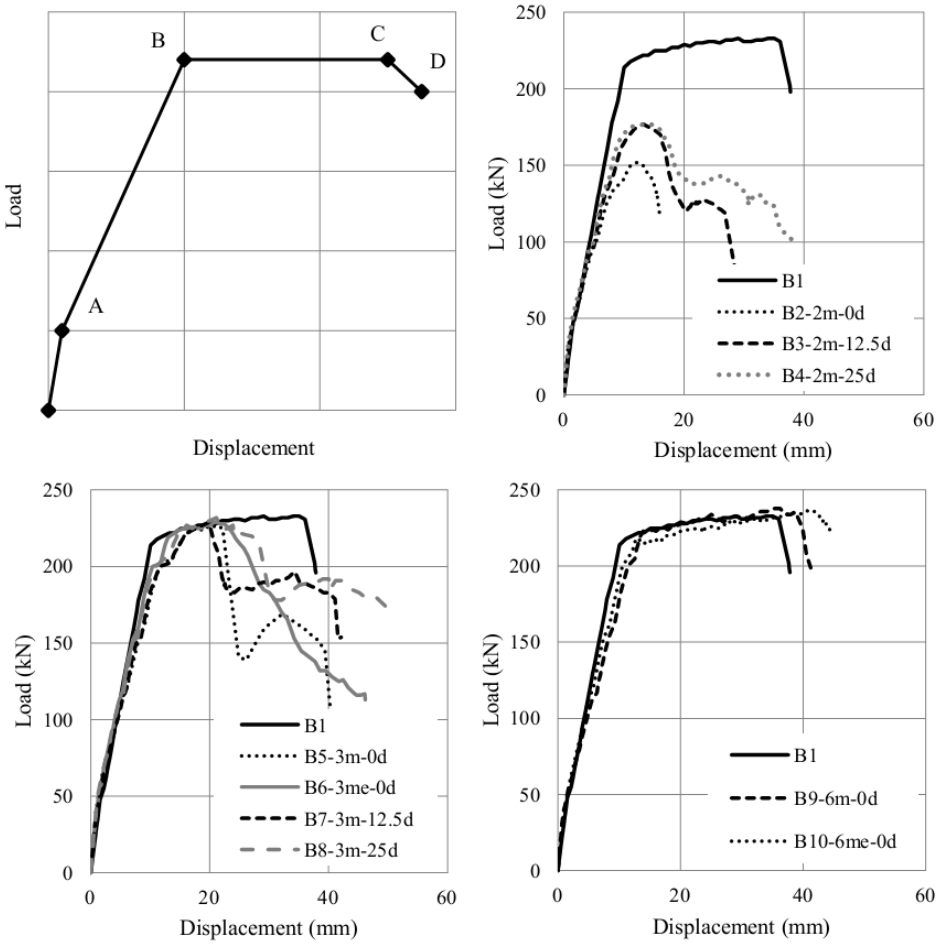

Figure 5. Load-displacement curves of beams

The stiffness of each beam is evaluated as the gradient of the load-displacement curve at each specified load or displacement. Figure 6 shows the relationship between load and stiffness obtained in this way from the load-displacement curves. A three-phase relationship can be discerned. The first phase is characterized by a marked fall in stiffness as the first cracks appear. Then the second phase begins once the cracks have stabilized; that is, when no new cracks are forming and load increments contribute to growth in crack length and width. In this phase, it seems that the stiffness decrease is negligible for the control beam, but notable for the beams using mechanical splices. Finally, the third phase is characterized by a sharp decrease in stiffness until collapse of the beam. It is very clear that, prior to cracking, beams using mechanical splices have greater stiffness than the control beam. This is because of the higher reinforcement ratio at the cross sections of the beams with mechanical splices. Upon cracking, the stiffness of the control beam falls slightly. Meanwhile, the beams using mechanical splices experience distinct degradation of flexural stiffness due to the gradual slippage of the steel bars from the couplers. The rate of degradation depends on bar embedment length in the couplers, in the order MS-2m, MS-3m, MS-6m.

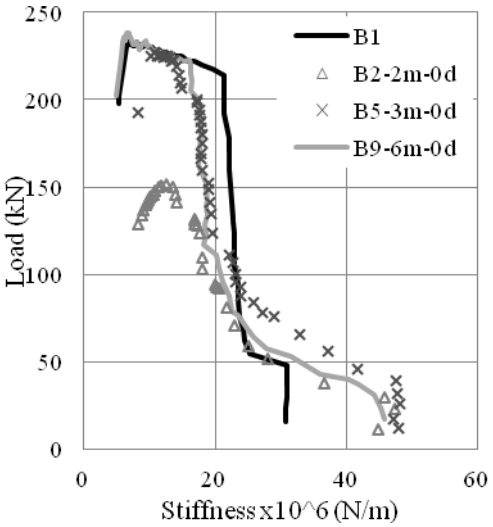

Figure 6. Stiffness of beams

Table 3 shows the beam test results. Failure is defined as in Eurocode 8 at the point when the load falls to 85% of the maximum load (or 15% reduction in load carrying capacity of RC elements).

Table 3. Beam test results

Beam	Yield		Ultimate		Failure		P_u/P_u (control beam)	μ
	P_y, kN	d_y, mm	P_u, kN	d_u, mm	P_f, kN	d_f, mm		
B1	214	10.05	233	35.03	198	37.77	1.00	3.76
B2-2m-0d	-	-	152	12.18	129	15.64	0.65	-
B3-2m-12.5d	-	-	177	13.23	150	17.28	0.76	-
B4-2m-25d	-	-	177	14.41	150	18.46	0.76	-
B5-3m-0d	191	10.82	227	21.09	193	23.18	0.97	2.1
B6-3me-0d	189	9.46	229	21.20	195	27.70	0.98	2.9
B7-3m-12.5d	163	8.92	229	19.84	193	22.07	0.98	2.5
B8-3m-25d	194	10.23	232	21.12	197	29.24	1.00	2.9
B9-6m-0d	163	9.32	238	36.27	202	40.99	1.02	4.4
B10-6me-0d	200	10.56	237	41.02	201	45.79	1.02	4.3

Notes: P_{cr} = cracking load; P_y, P_u, P_f = yield, ultimate, and failure loads; d_y, d_u, d_f = yield, ultimate, and failure displacements; μ = ductility index;

Beams using these MS-2m splices (B2-2m-0d, B3-2m-12.5d, B4-2m-25d) had notably lower load carrying capacities than the control beam. In particular, beam B2-2m-0d reached only 65% of the ultimate load of the control beam. For beams B3-2m-12.5d and B4-2m-25d, where the MS-2m splices were staggered, load carrying capacities were about 75% that of the control beam and 10% higher than that of beam B2-2m-0d. Thus, the staggering of the mechanical splices has a clear effect. The other beams (B5-3m-0d, B6-3me-0d, B7-3m-12.5d, B8-3m-25d, B9-6m-0d, B10-6me-0d) reached the yield load and had almost the same load carrying capacity as the control beam.

The deformability of beams before significant loss of strength occurs is estimated using the ductility index μ. The index is calculated by dividing the displacement at failure by that at yield. A minimum ductility index of 3.0 is generally required in the ACI 318-05 Code. The ductility indexes of the test beams are shown in Table 3. The behavior of beams B2-2m-0d, B3-2m-12.5d, B4-2m-25d was brittle. In the beams with MS-3m splices (B5-3m-0d, B7-3m-12.5d, B8-3m-25d), ductile behavior was observed. Beam B8-3m-25d (splices staggered by 25d+l) had a ductility index of 2.9 and beam B7-3m-12.5d (splices staggered by 12.5d+l) had an index of 2.5, while beam B5-3m-0d (no staggering) was 2.1. This demonstrates that the ductility index is proportional to the amount of stagger of the mechanical splices. The ductility index also increases when epoxy resin is injected into the coupler. Beam B6-3me-0d, which has non-staggered MS-3me splices (with epoxy), exhibited greater ductility than the beams using MS-3m splices (B5-3m-0d, B7-3m-12.5d, B8-3m-25d). In contrast, the ductility indexes of beams B5-3m-0d, B6-3me-0d, B7-3m-12.5d, B8-3m-25d, using splices with 3-thread embedment, did not meet the minimum requirements of the ACI code. Beams B9-6m-0d and B10-6me-0d, using properly embedded splices, had almost the same ductility as the control beam and satisfy the requirements of the ACI code.

3.3.2. Cracking behavior

Table 4. Maximum crack widths of beams

Beam	At service load	At P = 200 kN	
	w_{ser}, mm	w_b, mm	w_{sp}, mm
B5 - 3m - 0d	0.21	0.20	0.41
B6 - 3me - 0d	0.24	0.30	0.47
B7 - 3m - 12.5d	0.16	0.17	0.36
B8 - 3m - 25d	0.20	0.13	0.42
B9 - 6m - 0d	0.25	0.21	0.40

Notes: w_{ser} = max. crack width at service load; w_b = max. crack width at bar; w_{sp} = max. crack width at splices

Crack widths at the position of the steel bars are shown in Table 4. The service load is defined as 1/1.6 of the ultimate load. In the beams using mechanical splices, when the applied load reached the cracking moment, flexural cracks occurred simultaneously at both ends of the mechanical splices due to the reduced concrete cover in this region. Maximum crack widths of the test beams at the service loads were in all cases smaller than the allowable crack width (0.3 mm) as stipulated by the

ACI code. At a higher load (P = 200 kN), wide cracks opened near the mechanical splices as compared to those at other locations.

Figure 7 shows mid-spans of all beams at failure. Cracks are concentrated near the mechanical splices. There are fewer cracks in beams B2-2m-0d, B3-2m-12.5d, B4-2m-25d than in the control beam and other beams (B5-3m-0d, B6-3me-0d, B7-3m-12.5d, B8-3m-25d, B9-6m-0d, B10-6me-0d). This can be attributed to the large amount of slippage of steel bars from the coupler in MS-2m splices.

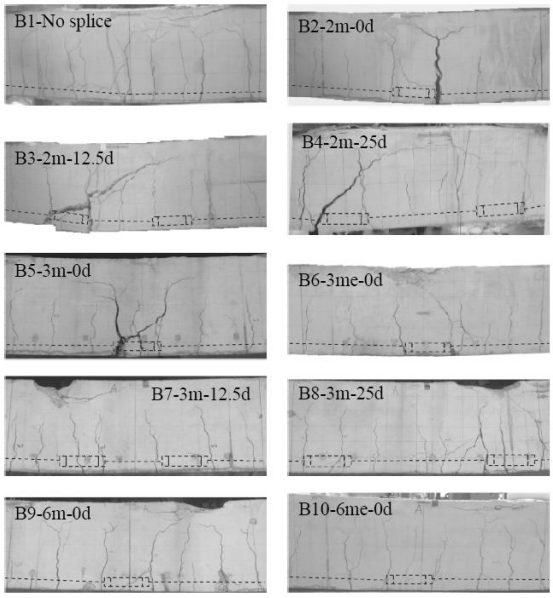

Figure 7. Crack patterns of beams

4. A NEWLY DEVELOPED CORRECTIVE SPLICE FOR IMPROVING IMPROPERLY INSTALLED MECHANICAL SPLICES

If an improperly formed splice is found, it is removed by cutting the bars and a new splice is installed. However, it is sometimes impossible to carry out this work because of construction site conditions. In this study, we develop a new corrective splice that brings a mechanical splice with insufficiently embedded bars up to the strength of a sound one.

4.1. Configuration

The configuration of the newly proposed corrective splice is shown in Figure 8. It uses for improving quality of the improperly installed mechanical splices studied in the previous sections. The corrective splice consists of two steel semi-cylinders that can be assembled by using bolts. Total length of the corrective splice is 400 mm. The outer diameter of the corrective splice is 50.8 mm and its thickness is 12 mm. The inner surface of corrective splice is grooved so as to increase bonding with the grout. On the upper semi-cylinder, two holes with diameter of 20 mm are drilled for grout injection. Another four tapped holes with diameter of 10 mm are drilled at the both semi-cylinders for inserting bolts to restrain the slippage of reinforcing bars from the mechanical splices and keep the bars stable during grout injection.

For installation, the improperly formed splice and bars are covered by the corrective splice. Four bolts without head are inserted into the tapped holes and tighten. The bolts are inserted fully into the tapped holes in order not to affect the concrete cover outside the corrective splice. High-strength grout (>80 MPa) is filled into the corrective splice to create a bond between the corrective splice and the original one and the bars. The bars are spliced based on three restrain factors included the strength of the improperly installed mechanical splice, the bond force of the grout and the force created by the four bolts.

The performance of the corrective splice depends on bond forces between the grout and the corrective splice, the original splice and the bars. The bolts are used to hold the steel bar firmly at the center of the corrective splice during grouting. The length of the corrective splice is set so as to ensure failure of the steel bar outside the corrective splice region. No additional strength is expected from the bolts.

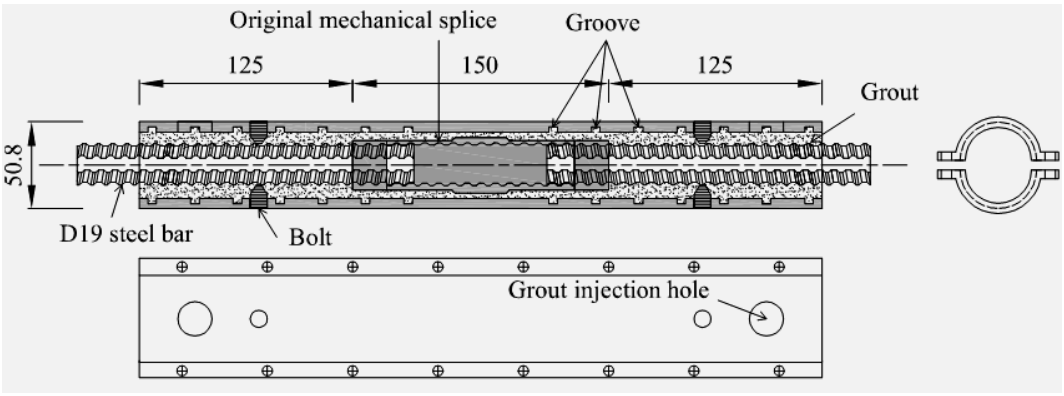

Figure 8. Structure and dimensions of the corrective splice

4.2. Tensile test

4.2.1. Specimens and set-up

A specimen using a newly developed corrective splice fitted over a two-thread embedment length mechanical splice was prepared (named as CS-2m). For comparison purpose, another specimen using a newly developed corrective splice in which plain steel bars with 200 mm insertion length was installed (named as CS-200). After injecting grout into the corrective splice, three grout cylinders with 25 mm in diameter and 50 mm in height were prepared to determine the compressive strength of the grout. Strain gauges were attached along the corrective splice and the steel bars to measure the strain distribution. Slip of the steel bars from the corrective splice was measured by two pairs of linear variable differential transformer. The specimen was gripped in the tensile testing machine. Tensile load was applied monotonically until the steel bars slipped out from the corrective splice or rupture of the steel bars. The test setup is shown in Figure 9.

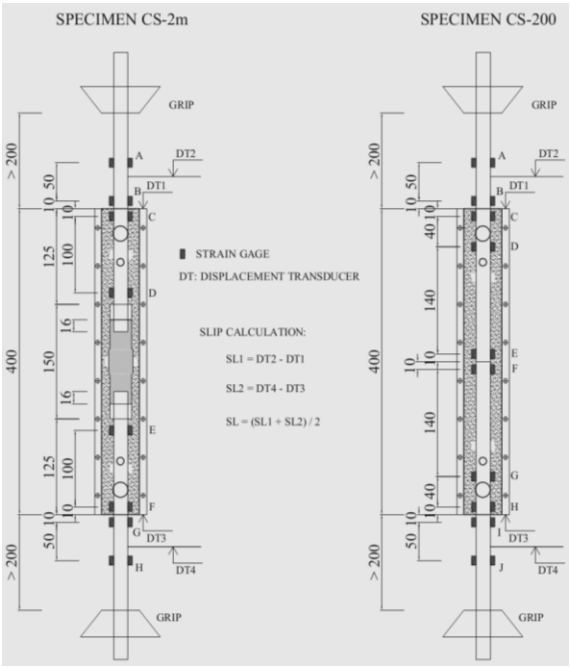

Figure 9. Tensile test setup for the corrective splice

4.2.2. Test results

The test results of the corrective splices are compared to those of the MS-2m and the plain D19 bar. Figure 10 shows the stress-strain curves of specimens CS-2m, CS-200, the MS-2m splice alone, and the D19 bar. The strains in specimens CS-2m and CS-200 are obtained from strain gauges attached at a point of 10 mm from the corrective splice. The strain in MS-2m is also taken 10 mm from the mechanical splice. Stresses are calculated by dividing the tensile load by the nominal area of the plain D19 bar (equals to 286.2 mm^2). In the case of MS-2m mechanical splice, the strain could only develop up to maximum strain of 1570 με and then the steel bar was slipped out. In the case of specimen CS-200, the strain can develop yield strain of the D19 bar but with lower stiffness. Failure of specimen CS-200 is also slippage of the steel bar from the corrective splice. For the case of specimen CS-2m, the strain develops the same as the plain D19 bar and the specimen CS-2m failed due to bar rupture outside the corrective splice, which means that tensile strength of specimen CS-2m is equal to that of the plain D19 bar.

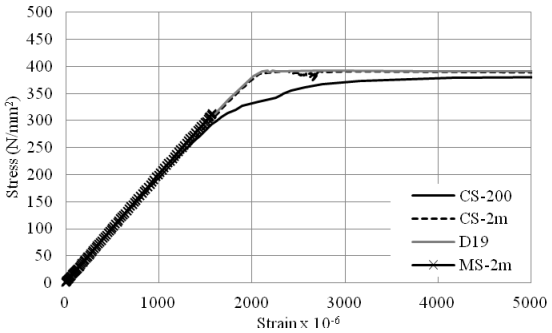

Figure 10. Stress-strain curve of a corrective splice

Figure 11 shows the slips of specimens CS-2m and CS-200 until yielding of the steel bar. Due to the capacity of the LVDTs, the slip after yielding of the steel bar could not be measured. As can be seen, the slip of specimen CS-2m is very small compared to that of the specimen CS-200. The strength of the improperly installed mechanical splice contributes well to performance of the corrective splice. It confirms the advantages of utilizing the improperly installed mechanical splice instead of removing it.

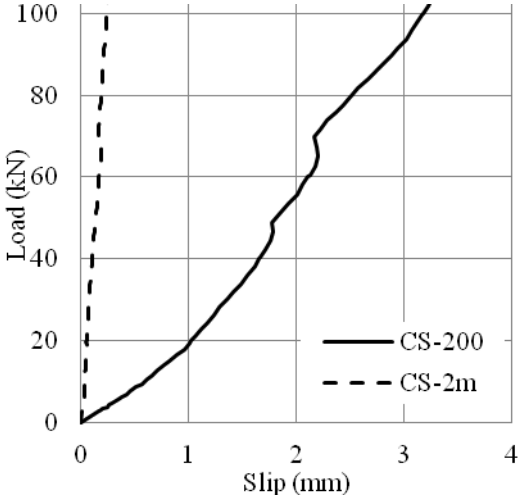

Figure 11. Slip of the corrective splice test

Table 5 shows the detail of the test results. Specimen CS-200 has lower ultimate strength than the plain D19 bar and failed due to slippage of the

steel bar from the corrective splice. Meanwhile, specimen CS-2m presents the same behavior as the D19 bar on ultimate strength and the failure mode (failure of the bar away from the corrective splice). Comparing the result of specimen CS-2m and CS-200, it can be seen that the restrain force by the improperly installed mechanical splice contributes not small amount to the quality of the corrective splice. With the same corrective splice, the one fitting over the improperly installed mechanical splice has a better performance in the one using for the plain steel bars (both in stiffness and ultimate strength).

Table 5. Tensile test results of a corrective splice

Specimen	f_u (N/mm^2)	$f_u / f_{y(D19)}$	Failure mode
D19 bar	546	143%	Bar rupture
MS-2m	240	63%	Bar slippage
CS-200	494	130%	Bar slippage
CS-2m	561	148%	Bar rupture

It can be concluded from the tensile test results that the corrective splice improves the performance of an improperly installed mechanical splice in which the bars are insufficiently embedded in the coupler.

4.3. Beam tests

4.3.1. Specimens and test set up

Table 6. Corrective splice beam tests

Beam	Note	f'c, N/mm^2	Number of principal bars
B1	No splice	36.2	4
B11	2MS-2m+2MS-6me	36.1	4
B12	2CS-2m+2MS-6me	35.2	4
B13	No splice	30.8	3
B14	3CS-2m	30.7	3

In order to investigate the mechanical behavior of reinforced concrete members with improperly installed mechanical splices that were subsequently improved using corrective splices, four reinforced concrete beams were prepared. The test variables of these beams are shown in Table 6 エラー! 参照元が見つかりません。. Beam B1, with results taken from the previous beam tests, is the control beam. Beam B11 was prepared for comparison purpose, two MS-2m splices and two MS-6me splices were installed in four reinforcing bars. In beam B12, two corrective splices were used to improve two MS-2m splices, while the other two splices were MS-6me. Beam B13 had three continuous steel bars as a control. In beam B14, three corrective splices were used to improve three MS-2m splices. Mechanical splices and corrective splices were located at the mid span of each beam. Beam dimensions, reinforcement detail, instrumentation, test set-up and loading method were the same as shown in the previous tests.

4.3.2. Test results

Figure 12 shows the load-displacement curves of the test beams. It can be seen that beam B11 with the MS-2m and MS-6me splices, had a lower load carrying capacity than the control beam B1 and could not reach the yielding stage. The reason is that the improperly formed MS-2m splices in beam B11 failed prior to the yielding of the reinforcing bars. Beam B12, containing MS-6me splices and corrected MS-2m splices, shows good improvement compared to beam B11. It exhibits a little higher load carrying capacity than the control beam B1 with almost the same ultimate displacement. Beam B14 in which three corrective splices are fitted over MS-2m splices shows the same load carrying capacity as the control beam B13 with three continuous steel bars. The ultimate displacement of beam B14 is larger than beam B13, which shows that ductile of beam B14 is also larger than that of beam B13.

For clearly observation, the stiffness change of the beams was shown in Figure 13. The three-phase behavior of stiffness as shown in the previous tests was observed. For beam B11, it has a higher stiffness at the early stage of loading (no crack appeared) than the control beam but there is a significant decrease in stiffness of this beam at phase 2 meanwhile the stiffness of the control beam decreases slightly. For beams B12 and B14 which have corrective splices, the stiffness is higher than the control beam in all three phases although the rate of degradation in beams B12 and B14 is higher than the control beam. The reason can be attributed to the higher steel-to-concrete ratio at the corrective splices section.

Table 7 summarizes the test results. Yielding of beams B1 and B12 occurred at 10 mm displacement with about 210 kN applied load. However, in beam B11 using MS-2m mechanical splices, yielding load is 169 kN which is lower than beams B1 and B12. It is because of the MS-2m mechanical splices failed due to slippage of the reinforcing bars from the couplers and the redistribution of the moment makes the reinforcing bars using MS-6me subjected to higher load and yielded soon. Beam B12 exhibits higher load

carrying capacity than the control beam B1 (239 kN compared to 233 kN) meanwhile beam B11 has much lower strength (185 kN). Failure of beam B11 occurred very soon, at 19 mm displacement, that of beam B1 is 38 mm and beam B12 is 41 mm. Therefore, the displacement ductility index of beam B12 is higher than the control beam B1. For the case of beams B13 and B14, they have almost the same yield load and ultimate load. Beam B14 also has a higher ductility than the control beam B13.

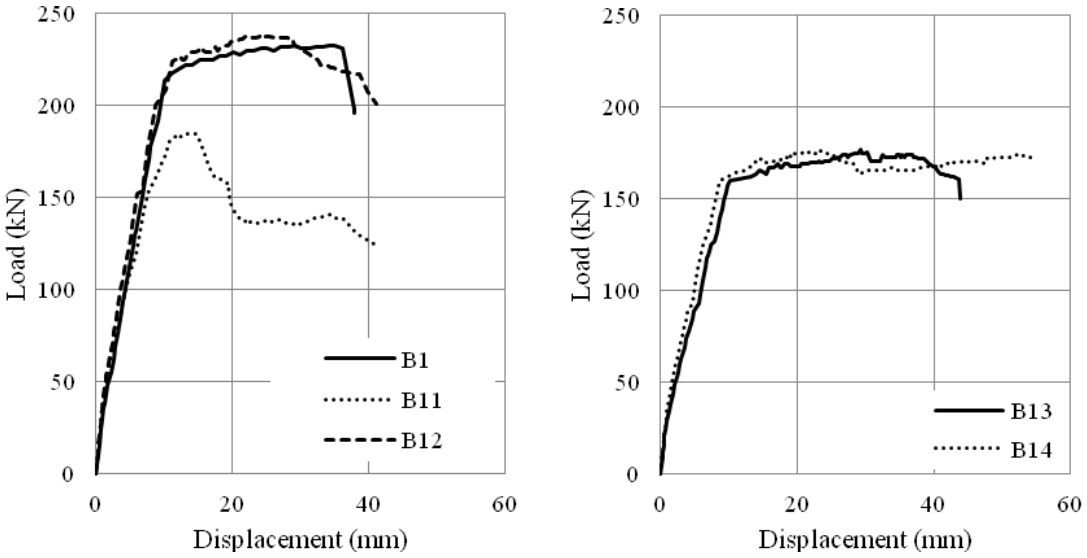

Figure 12. Load-displacement curves of the test beams

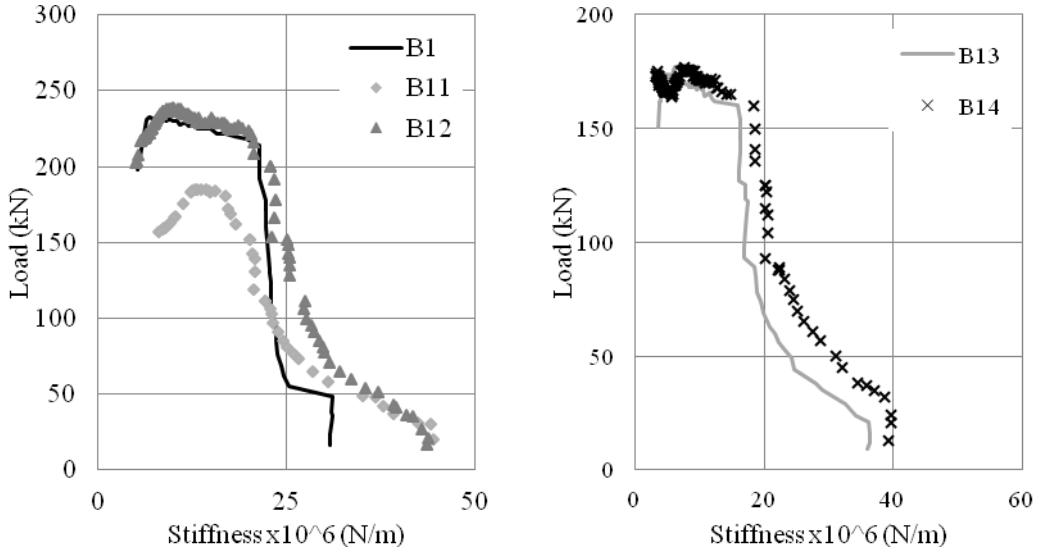

Figure 13. Stiffness of beams using corrective splices

Table 7. Test results of beams using corrective splices

Beam	Yield		Ultimate		Failure		Pu/ Pu (control beam)	Ductility (%)
	P_y (kN)	d_y (mm)	P_u (kN)	d_u (mm)	P_f (kN)	d_f (mm)		
B1	214	10.05	233	35.03	198	37.77	1.00	3.758
B11	169	9.62	185	14.58	157	19.49	0.79	2.027
B12	209	10.13	239	24.29	203	40.62	1.03	4.010
B13	149	9.20	177	29.21	150	43.92	1.00	4.777
B14	150	8.11	177	23.27	173	55.05	1.00	6.788

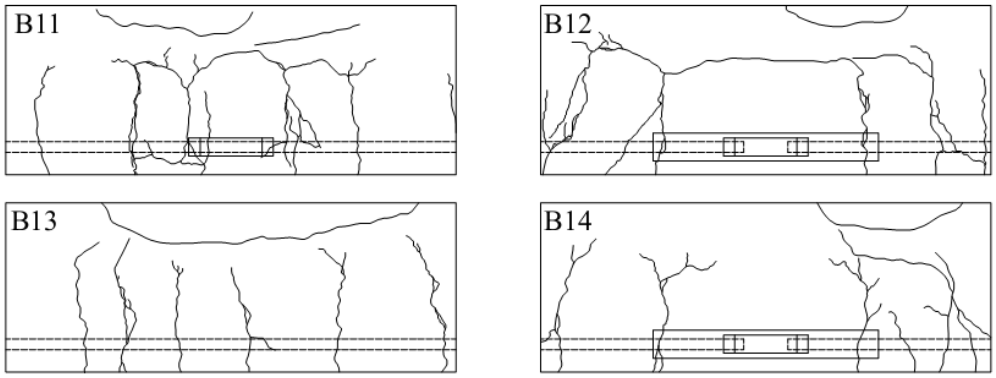

Figure 14. Crack patterns in the corrective splice beam tests

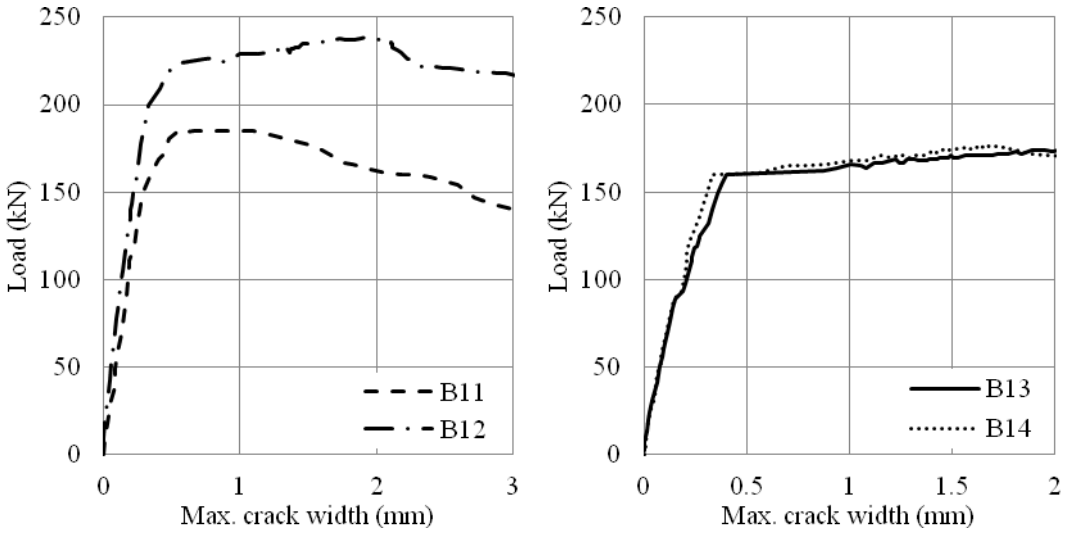

Figure 15. Crack widths development in the test beams

Figure 14 shows the crack patterns of the four test beams at failure. It can be seen clearly that the beams fitted with corrective splices have few cracks compared to the others because no cracks form over the length of the corrective splices.

Figure 15 shows the development of crack widths in the test beams. In beam B12 using corrective splices, the slippage of the reinforcing bars from the mechanical splices is more restrained by using the corrective splices so that the cracks opened narrower than those of beam B11 using M2-2m mechanical splices. This improvement is confirmed in the case of beam B14 using corrective splices fitting over MS-2m mechanical splices compared to beam B13 using continuous reinforcing bars, there is almost no difference between the crack width development of the two beams as can be seen in the figure.

5. CONCLUSION

The mechanical properties of mechanical splices with insufficient steel bar insertion into the couplers were experimentally investigated along with the influence of such splices on the behavior of RC beams. The effectiveness of a corrective splice newly developed to improve such improperly installed splices was also studied. The following conclusions can be drawn from this work:

- A mechanical splice in which the steel bars are insufficiently embedded into the coupler fails through slippage of the steel bars from the coupler. Such splices fail to reach the ultimate strength of the steel bar.
- A beam using mechanical splices in which the steel bars are insufficiently embedded into the coupler performs poorly, while a beam fabricated using properly formed mechanical splices exhibits almost the same behavior as a control beam using no mechanical splices.
- The injection of epoxy and a staggered arrangement can enhance the performance of mechanical splices in which the steel bars are insufficiently embedded in the coupler.
- Staggering mechanical splices by 25d+l, as stipulated by the JSCE's standard, is conservative. Properly formed mechanical splices can be used at the same cross section (without staggering) without

significant deviation from the behavior of a control beam. Further studies are necessary to determine reasonable specifications for this situation.
- The newly developed corrective splice improves the mechanical properties of a mechanical splice in which the steel bars are insufficiently embedded in the coupler as well as those of the RC beams.
- When a corrective splice is used in a RC member, the concrete cover over the length of the corrective splice is reduced as compared with a conventional splice. Therefore a corrective splice is suitable for use on the inner bars in a RC member.

ACKNOWLEDGMENTS

This study was carried out with the support of Grant-in-Aid for Scientific Research (B), Japan. The authors would like to acknowledge members of Structural Material Laboratory of Saitama University, Japan for their support. Special appreciation is extended to the staff of Tokyo Tekko Company Ltd. for their contributions during various stages of the experimental program.

REFERENCES

ACI Committee 439, "Types of Mechanical Splices for Reinforcing Bars," ACI Committee Report, ACI 439.3R-07, March 2007.

Concrete Reinforcing Steel Institute, "Reinforcing bars: anchorages and splices," 2008.

M. Patrick, P.A. Berry and R.Q. Bridge, "Strength and Ductility of Mechanically Spliced Bars", Concrete Institute of Australia, February 13, 2011.

Stephen P. Rowell, Clifford E. Grey, Stanley C. Woodson, and Kevin P. Hager, "High Strain-Rate Testing of Mechanical Couplers", U.S. Army Corps of Engineers Report ERDC TR-09-8, Sept. 2009, pp. 73.

Keith L. Coogler, Kent A. Harries, and Marcella Gallick, "Experimental Study of Offset Mechanical Lap Splice Behavior," ACI Structural Journal, V. 105, No. 4, July-August 2008, pp. 478-487.

Aizat Alias, Mohammad Amirulkhairi Zubir, Khairul Anuar Shahid, and Ahmad Baharuddin Abd RAhman, "Structural Performance of Grouted Sleeve Connectors With and Without Transverse Reinforcement For Precast Concrete Structure," Procedia Engineering 53 (2013), pp. 116–123.

Peter O. Jansson, "Evaluation of Grout-Filled Mechanical Splices for Precast Concrete Construction", Research Report R-1512, Michigan Department of Transportation MDOT, Michigan, May 2008.

Allen J. Hulshizer, Joseph J. Ucciferro, and George E. Gray, "Mechanical Reinforcement Couplings Meet Demands of Strength and Constructibility", Concrete International, V. 16, January 1994, pp. 47-52.

Mete A. Sozen and William L. Gamble, "Strength and Cracking Characteristics of Beams with #14 and #18 Bars Spliced with Mechanical Splices," ACI Journal, Dec. 1969, pp. 949-956.

R. Joseph Reetz, Malte von Ramin, and Adolfo Matamoros, "Performance of mechanical splices within the plastic hinge region of beams subject to cyclic loading," 13th World Conference on Earthquake Engineering, Vancouver, B.C., Canada, August 1-6, 2004, Paper No. 1073.

Zachary B. Haber, M. Saiid Saiidi, and David H. Sanders, "Seismic Performance of Precast Columns with Mechanically Spliced Column-Footing Connections", ACI Structural Journal, V. 111, No.3, May-June 2014, pp. 639-650.

S. Sritharan, J. Ingham, M. Priestley, and F. Seible, "Design and Persormance of Bridge Cap Beam/Column Using Headed Reinforcement and Mechanical Couplers", ACI Special Volume on Development of Seismic Steel Reinforcement Products and Systems, ACI SP-184, 1999, pp. 7-22.

Japan Reinforcing Bar Joints Institute, "Standard specification for splice of steel bars – Mechanical splice", 2009 (in Japanese).

ACI Committee 318, "Building Code Requirements for Structural Concrete (ACI 318-05) and Commentary," American Concrete Institute, 2005.

Japan Society of Civil Engineers, "Standard Specification for Concrete Structures – Design", 2007.

R. Park and T. Paulay, "Reinforced concrete structures", Wiley, USA, 1975.

European Committee for Standardisation, "Eurocode 8. EN 1998-1. Design of structures for earthquake resistance. Part 1: General rules, seismic actions and rules for buildings," 2004.

ACI Committee 224, "Control of Cracking in Concrete Structures," American Concrete Institute, 2001.